

# Electronic Absorption and Resonance Raman Signatures of Hyperporphyrins and Nonplanar Porphyrins

Ingar H. Wasbotten,<sup>†</sup> Jeanet Conradie,<sup>‡</sup> and Abhik Ghosh<sup>\*,†</sup>

*Institute of Chemistry, Faculty of Science, University of Tromsø, N-9037 Tromsø, Norway, and  
Department of Chemistry, University of the Free State, 9300 Bloemfontein, Republic of South Africa*

*Received: December 5, 2001; In Final Form: December 3, 2002*

We have carried out a broad survey of tetraphenylporphyrin derivatives in relation to their possible hyperporphyrin character. The majority of the free-base tetraphenylporphyrins studied, i.e., TArPH<sub>2</sub>; Ar = *p*-X-C<sub>6</sub>H<sub>4</sub>, where X = CH<sub>3</sub>, H, F, CF<sub>3</sub>, and NO<sub>2</sub>, when dissolved in trifluoroacetic acid (i.e. when centrally diprotonated), exhibit red-shifted “hyperporphyrin” spectra. The “hyper” features are attributable to phenyl-to-porphyrin charge-transfer transitions. However, certain free-base tetraphenylporphyrins with extremely electron-deficient phenyl groups, such as TPFPPH<sub>2</sub>, do not exhibit hyperporphyrin spectra in trifluoroacetic acid solution. Certain anionic tetraphenylporphyrin derivatives such as T(*p*-OH-P)PH<sub>2</sub> or Ni[T(*p*-OH-P)P] dissolved in methanolic Bu<sub>4</sub>NOH also qualify as hyperporphyrins. The hyper transitions in these cases involve charge transfer from anionic phenolate substituents to the neutral porphyrin core. This study also presents a first systematic resonance Raman spectroscopic exploration of hyperporphyrins. Comparison of the Soret-resonant Raman spectra of various normal, hyper-, and hypso- tetraphenylporphyrin derivatives indicates that the former two categories generally exhibit a more intense  $\nu_1$  band, which is the fully symmetric C<sub>meso</sub>–C<sub>phenyl</sub> stretching vibration, relative to hypso-porphyrins such as square-planar nickel tetraarylporphyrins. We have also reinvestigated recent reports of large red shifts observed for the electronic spectra of saddled porphyrins in polar solvents, an effect attributed to increased N–H···solvent hydrogen bonding in polar solvents. Interestingly, we find that such solvent-induced red shifts are observed for the relatively electron-deficient porphyrin Br<sub>8</sub>TPPH<sub>2</sub>, Cl<sub>8</sub>TPPH<sub>2</sub>, and OETNPH<sub>2</sub> but not for the relatively electron-rich OETPPH<sub>2</sub>. Resonance Raman spectra of these saddled porphyrins in different solvents reveal little shift in the high-frequency marker bands, which is consistent with little change in macrocycle conformation with solvent polarity. The observed solvent-induced red shifts in the electronic spectra therefore appear to reflect a largely electronic (as opposed to conformational) effect of N–H···solvent hydrogen bonding in polar solvents. Finally, we also present a chronological summary of the controversial question as to whether nonplanar deformations are actually responsible for the red-shifted electronic spectra of the majority of nonplanar porphyrins.

## Introduction

The importance of porphyrin-type pigments in photobiological processes such as photosynthesis has led to a vast body of electronic absorption and other spectroscopic studies of these compounds.<sup>1</sup> Recent applications of porphyrinoids in photodynamic therapy<sup>2,3</sup> and as photoconductors<sup>4,5,6</sup> have provided a further stimulus for such studies. In particular, much interest has focused, both from the point of view of photodynamic therapy and otherwise, on porphyrin derivatives exhibiting unusually red-shifted absorption spectra; these derivatives include certain transition metal porphyrins, nonplanar porphyrins, and nontransition-metal hyperporphyrins. Certain iron(IV) corrole derivatives have been found to exhibit “hyper” (defined below) spectra and split Soret bands remarkably similar to those exhibited by chloroperoxidase compound II.<sup>7,8,9</sup> These and other findings have led to a general interest in understanding the factors bringing about red-shifted optical spectra in porphyrin deriva-

tives. Against this context, we present here a broad electronic absorption and resonance Raman spectroscopic survey of tetraphenylporphyrin derivatives that exhibit hyper optical spectra.

The various features in the electronic absorption spectra of “normal” porphyrin are all generally ascribable to  $\pi$ – $\pi^*$  transitions of the porphyrin ring. The electronic absorption spectra of hyperporphyrins exhibit prominent additional bands<sup>10</sup> in the region  $\lambda > 320$  nm which are not porphyrin<sup>10</sup>  $\pi$ – $\pi^*$  transitions. “Hyper” spectra are characterized by a red-shifted Soret band and one or more new, intense, broad bands in the visible and far red. These extra features are often due to charge transfer (CT) transitions such as from porphyrin-to-metal(d) or porphyrin-substituent-to-porphyrin or otherwise. Many experimental porphyrin researchers routinely encounter hyperporphyrins, often in connection with washing porphyrin-stained laboratory glassware with acid. Acid immediately turns a reddish tetraphenylporphyrin stain brilliant green, although octaethylporphyrin does not undergo a similar visual change on acidification. The reason is that protonated tetraphenylporphyrin is a hyperporphyrin.

Here we revisit hyperporphyrins with three specific goals.

\* Author to whom correspondence should be addressed. E-mail: abhik@chem.uit.no.

<sup>†</sup> University of Tromsø.

<sup>‡</sup> University of the Free State.

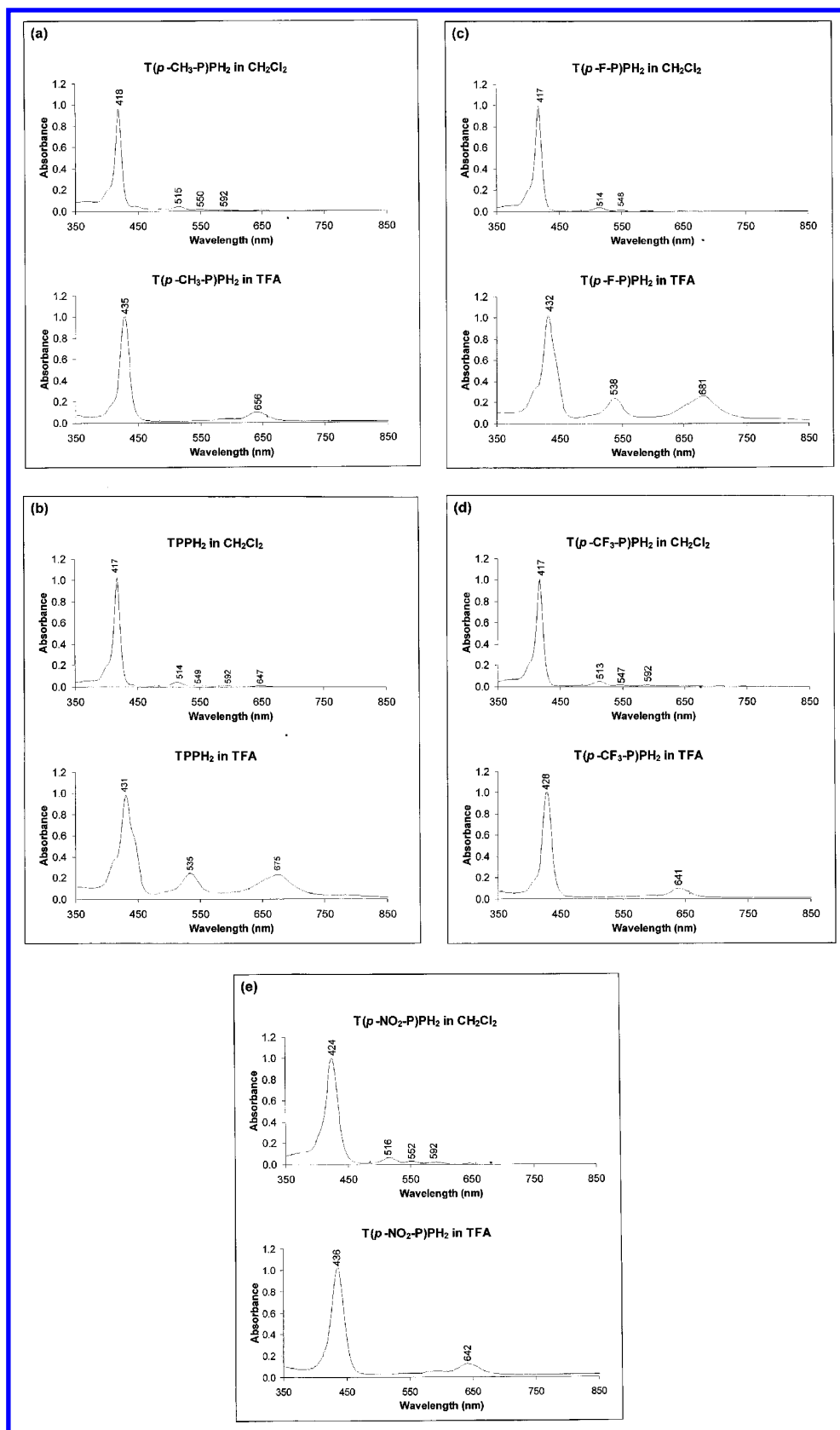


**Figure 1.** Electronic absorption spectra of selected tetraphenylporphyrins in dichloromethane and TFA. (a)  $T(p\text{-CH}_3\text{-P})\text{PH}_2$ , (b)  $\text{TPPH}_2$ , (c)  $T(p\text{-F-P})\text{PH}_2$ , (d)  $T(p\text{-CF}_3\text{-P})\text{PH}_2$ , and (e)  $T(p\text{-NO}_2\text{-P})\text{PH}_2$ .

First, we wanted to carry out a survey of the optical characteristics of a wide range of protonated free-base tetraarylporphyrins.

Second, we have examined the question as to whether anionic hyperporphyrins exist, i.e., free-base tetraphenylporphyrins with

a neutral porphyrin core and anionic substituted meso-phenyl groups.

Third, we wished to examine whether the different tetraphenylporphyrin derivatives with hyper spectra exhibit any common features in their resonance Raman spectra.

**TABLE 1: UV–Vis  $\lambda_{\text{Max}}$  (nm) and  $\log \epsilon$  for Tetraphenylporphyrins in Neutral (Usually Dichloromethane; Methanol for Ni[T(*p*-OH-*P*)P] and T(*p*-OH-*P*)PH<sub>2</sub>), Acidic (TFA), or Basic (12.5% Bu<sub>4</sub>NOH in Methanol) Solutions**

porphyrin	conditions	Soret band <sup>a</sup>		Q-bands							
		$\lambda$	$\log \epsilon$	$\lambda$	$\log \epsilon$	$\lambda$	$\log \epsilon$	$\lambda$	$\log \epsilon$	$\lambda$	$\log \epsilon$
TPPH <sub>2</sub>	neutral	417	5.68	514	4.30	549	3.96	592	3.84	647	3.80
TPPH <sub>2</sub>	acidic	431	5.36	535	4.76	675	4.72				
T( <i>p</i> -CH <sub>3</sub> - <i>P</i> )PH <sub>2</sub>	neutral	418	5.28	515	3.94	550	3.60	592	3.41		
T( <i>p</i> -CH <sub>3</sub> - <i>P</i> )PH <sub>2</sub>	acidic	435	5.23	656	4.42						
T( <i>p</i> -F- <i>P</i> )PH <sub>2</sub>	neutral	417	5.55	514	4.13	548	3.66				
T( <i>p</i> -F- <i>P</i> )PH <sub>2</sub>	acidic	432	5.35	681	4.76	538	4.73				
T( <i>p</i> -CF <sub>3</sub> - <i>P</i> )PH <sub>2</sub>	neutral	417	5.51	513	4.19	547	3.78	592	3.74		
T( <i>p</i> -CF <sub>3</sub> - <i>P</i> )PH <sub>2</sub>	acidic	428	5.61	641	4.61						
T( <i>p</i> -NO <sub>2</sub> - <i>P</i> )PH <sub>2</sub>	neutral	424	5.47	516	4.29	552	3.97	592	3.85		
T( <i>p</i> -NO <sub>2</sub> - <i>P</i> )PH <sub>2</sub>	acidic	436	5.73	642	4.82						
T( <i>p</i> -NH <sub>2</sub> - <i>P</i> )PH <sub>2</sub>	neutral	428	5.31	563	4.02	523	4.01	657	3.81		
T( <i>p</i> -NH <sub>2</sub> - <i>P</i> )PH <sub>2</sub>	acidic	429	5.43	639	4.90						
TPFPPH <sub>2</sub>	neutral	412	4.99	506	3.85	584	3.39				
TPFPPH <sub>2</sub>	acidic	423	5.53	571	4.23	622	4.15				
Br <sub>8</sub> TPPH <sub>2</sub>	neutral	468	5.31	744	4.20	626	4.13	571	3.88		
Br <sub>8</sub> TPPH <sub>2</sub>	acidic	485	5.29	751	4.87	585	4.86				
Cl <sub>8</sub> TPPH <sub>2</sub>	neutral	453	5.33	602	4.08	552	4.06	719	3.92		
Cl <sub>8</sub> TPPH <sub>2</sub>	acidic	475		724							
OETPPH <sub>2</sub>	neutral	457	5.17	555	3.94	600	3.85	701	3.81		
OETPPH <sub>2</sub>	acidic	459	5.39	683	4.53	563	4.22				
OETNPH <sub>2</sub>	neutral	427	4.88	531	4.12	572	3.75	614	3.75	667	3.35
OETNPH <sub>2</sub>	acidic	448		562		595		648			
T( <i>p</i> -OH- <i>P</i> )PH <sub>2</sub>	neutral	419	5.92	519	4.60	555	4.60	592	4.30		
T( <i>p</i> -OH- <i>P</i> )PH <sub>2</sub>	basic	443	4.96	592	4.18	679	3.96				
Ni[T( <i>p</i> -OH- <i>P</i> )P]	neutral	415	5.35	527	4.25	573	3.59				
Ni[T( <i>p</i> -OH- <i>P</i> )P]	basic	446	5.08	596	4.12	543	4.03				

<sup>a</sup> Only the Soret band with highest absorbance is listed.

We also make a few comments on nonplanar porphyrins which generally exhibit red-shifted optical spectra compared with common planar porphyrins. The exact cause of these red shifts has been the subject of much controversy<sup>11–5</sup> in recent years and we provide a summary of our current appreciation of this question.

Last, a number of free-base nonplanar porphyrins have been found to exhibit strongly red-shifted electronic spectra in polar solvents such as DMF and DMSO and the effects has been ascribed to hydrogen-bonding interactions involving the central NH groups and solvent molecules.<sup>16,17</sup> We have examined this phenomenon using resonance Raman spectroscopy.

**Methods.** Unless otherwise mentioned, all free-base porphyrins studied were purchased from Midcentury Chemicals, Inc. The  $\beta$ -octahalogeno-*meso*-tetraphenylporphyrins Br<sub>8</sub>TPPH<sub>2</sub> and Cl<sub>8</sub>TPPH<sub>2</sub> were obtained by demetalation of the corresponding Ni porphyrins<sup>18</sup> with H<sub>2</sub>SO<sub>4</sub>.  $\beta$ -Octaethyl-*meso*-tetranitroporphyrin, OETNPH<sub>2</sub>, was prepared as described in the literature.<sup>19</sup> All solvents employed in this study were of analytical grade and were further purified and distilled before use. UV–vis spectra were recorded on an HP 8453 spectrophotometer. Resonance Raman (RR) spectra were obtained with a Spex Jobin-Yvon double monochromator equipped with a liquid nitrogen cooled Spex Jobin-Yvon CCD 2000 detector and a Coherent Innova 70 Series mixed Ar–Kr laser. The laser line at 457.9 nm was used for most of the porphyrins. For Br<sub>8</sub>TPPH<sub>2</sub> in TFA, the line at 488.0 nm was used to obtain Soret-excited RR spectra. RR spectra of NiT(*p*-CF<sub>3</sub>-*P*)P and NiT(*p*-OH-*P*)P were obtained with the 406.0 nm of a Coherent Kr laser. All RR measurements were carried out on porphyrin solutions placed inside sealed glass capillaries. Sample integrity was monitored by UV–visible absorption spectroscopy immediately before and after the RR measurements. No sample photodegradation was apparent as a result of the laser irradiation.

## Results and Discussion

**(a) Electronic Absorption Spectra and the Question of Anionic Hyperporphyrins.** The Soret and Q-bands of most of

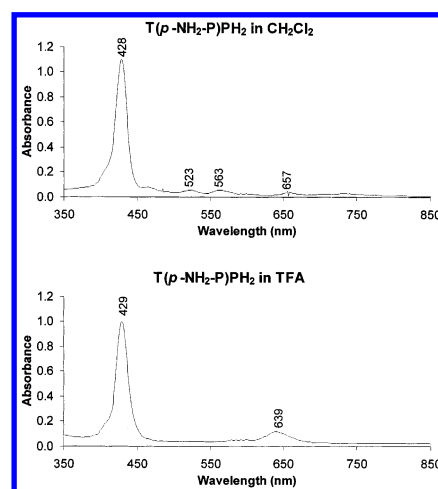


**Figure 2.** Electronic absorption spectra of T(*p*-NH<sub>2</sub>-*P*)PH<sub>2</sub> in dichloromethane and TFA.

the free-base tetraphenylporphyrins exhibit a significant red shift, i.e., hyper character, in trifluoroacetic acid (TFA), compared with dichloromethane solutions (Figure 1a–e and Table 1). Thus, the Soret band of a variety of free-base tetraphenylporphyrins (TArPH<sub>2</sub>; Ar = *p*-X-C<sub>6</sub>H<sub>4</sub>, where X = CH<sub>3</sub>, H, F, CF<sub>3</sub>, and NO<sub>2</sub>) exhibit a red shift of  $14 \pm 3$  nm in TFA, compared to dichloromethane solutions. These red shifts also parallel dramatic visual changes: the TFA solutions are brilliant green, compared with the reddish color of the dichloromethane solutions. As suggested by Gouterman and subsequently substantiated by means of semiempirical calculations,<sup>10,20</sup> the red shifts and the new Q-bands reflect phenyl-to-porphyrin CT transitions. Some exceptions to these generalizations as well as other detailed comments are as follows.

Tetrakis(*p*-aminophenyl)porphyrin (T(*p*-NH<sub>2</sub>-*P*)PH<sub>2</sub>), dissolved in TFA, does not exhibit a hyper spectrum (Figure 2). This is understandable because when the amino groups on the phenyl rings are protonated, phenyl-to-porphyrin CT transitions

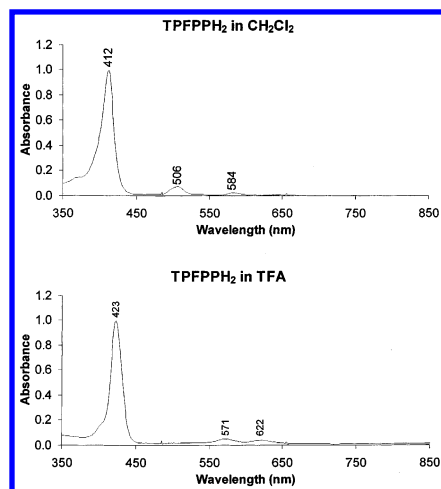


**Figure 3.** Electronic absorption spectra of TPFPPh<sub>2</sub> in dichloromethane and TFA.

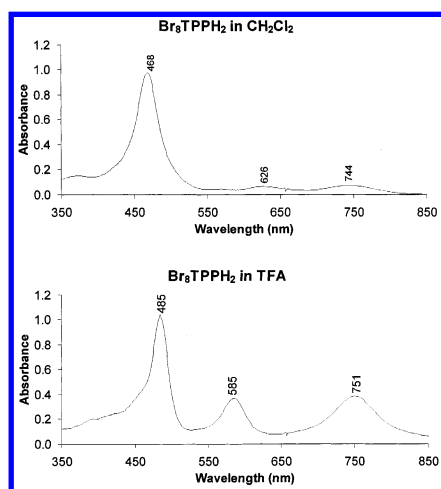


**Figure 4.** Electronic absorption spectra of Br<sub>8</sub>TPPh<sub>2</sub> in dichloromethane and TFA.

involving such electron-deficient phenyl groups are not expected in the optical spectrum. Gouterman and co-workers have described analogous behavior for tetra(*p*-dimethylaminophenyl)-porphyrin.<sup>20,21</sup>

Similarly, tetrakis(pentafluorophenyl)porphyrin (TPFPPh<sub>2</sub>), dissolved in TFA, also does not exhibit a typical hyper spectrum (Figure 3): although the Soret band in TFA shifts by 11 nm, relative to a dichloromethane solution, the Q-bands in TFA are relatively weak.

Compared with dichloromethane solutions, the Soret bands of Cl<sub>8</sub>TPPh<sub>2</sub> (Figure 5) and Br<sub>8</sub>TPPh<sub>2</sub> (Figure 4) in TFA are red-shifted by 22 and 17 nm, respectively. The Soret band of OETNPh<sub>2</sub> red-shifts by 21 nm in TFA relative to dichloromethane solution (Figure 6). Interestingly, the Soret band of  $\beta$ -octaethyl-*meso*-tetraphenylporphyrin, OETPPH<sub>2</sub>, red-shifts by only 2 nm in TFA, relative to a dichloromethane solution, although a Q-band intensifies significantly in TFA (Figure 7). We do not yet understand the reason for this different behavior of OETPPH<sub>2</sub> compared with the behaviors of the other saddled porphyrins studied.

To investigate whether anionic analogues of the above-mentioned cationic hyperporphyrins might exist, we have examined the deprotonation of free-base *meso*-tetrakis(*p*-hydroxyphenyl)porphyrin (T(*p*-OH-P)PH<sub>2</sub>) and nickel(II) tetrakis(*p*-hydroxyphenyl)porphyrin (Ni[T(*p*-OH-P)P]). To our knowl-

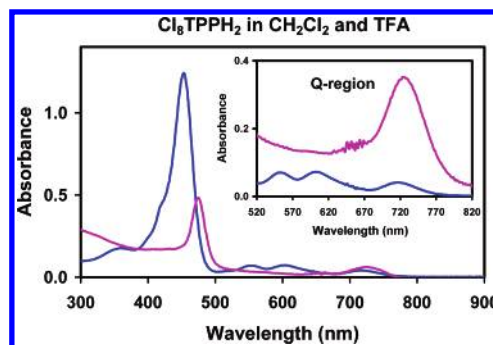


**Figure 5.** UV-vis spectra of the saddled free-base porphyrin Cl<sub>8</sub>-TPPh<sub>2</sub> in neutral dichloromethane (blue) and acidic TFA (magenta) solvents.

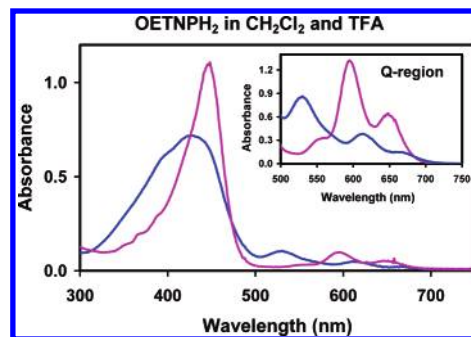


**Figure 6.** UV-vis spectra of the saddled free-base porphyrin OETNPh<sub>2</sub> in neutral dichloromethane (blue) and acidic TFA (magenta) solvents.

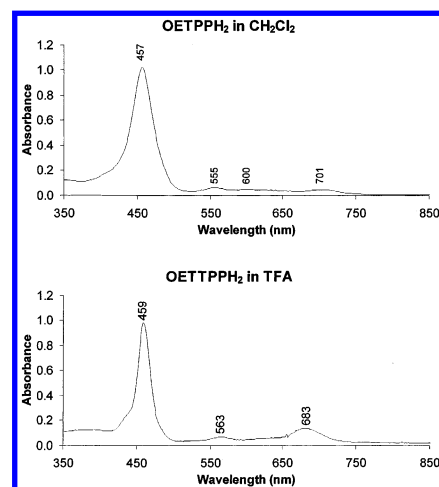


**Figure 7.** Electronic absorption spectra of OETPPH<sub>2</sub> in dichloromethane and TFA.

edge, Rohatgi-Mukherjee and co-workers<sup>22</sup> were the first to carry out a variant of this experiment although they did not describe the anionic species they generated as hyperporphyrins. When a speck of the ordinarily reddish T(*p*-OH-P)PH<sub>2</sub> or Ni[T(*p*-OH-P)P] is added to a few mL of a 12.5% methanolic solution of tetrabutylammonium hydroxide (Bu<sub>4</sub>NOH, from Merck), the solution turns brilliant green. The Soret bands of T(*p*-OH-P)PH<sub>2</sub> and Ni[T(*p*-OH-P)P] red-shift by 24 and 31 nm, respectively, in methanolic 12.5% Bu<sub>4</sub>NOH, relative to dichloromethane (Figure 8). The fact that the same effect is seen for both T(*p*-OH-P)PH<sub>2</sub> and Ni[T(*p*-OH-P)P] indicates that it results from deprotonation of the phenolic protons and not the NH protons of the free-base porphyrin.

Are the anionic derivatives of T(*p*-OH-P)PH<sub>2</sub> or Ni[T(*p*-OH-P)P] hyperporphyrins? We believe so. The hyper transitions in these cases involve CT from anionic phenolate substituents to

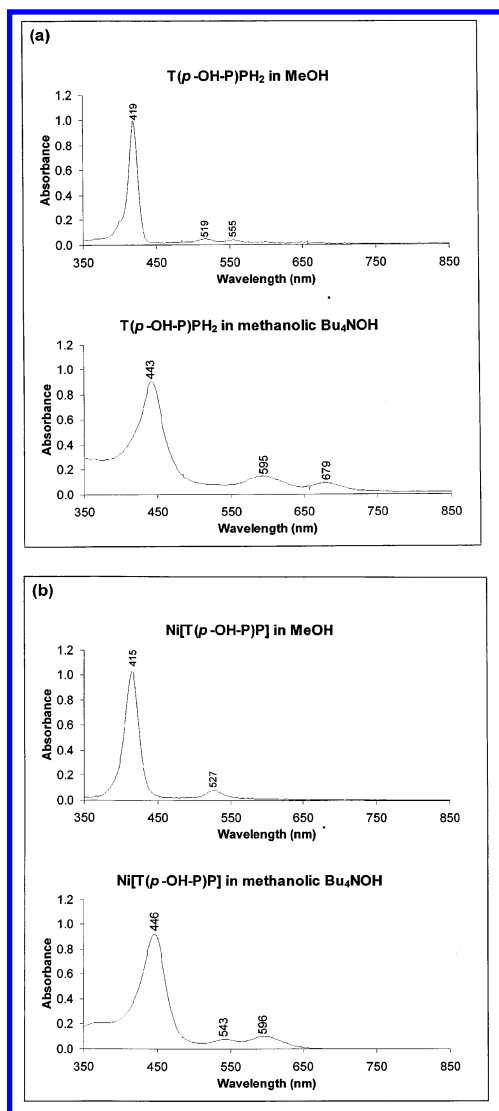


**Figure 8.** Electronic absorption spectra of (a)  $T(p\text{-OH-P})\text{PH}_2$  and (b)  $\text{Ni}[T(p\text{-OH-P})\text{P}]$  in methanol and methanolic 12.5%  $\text{Bu}_4\text{NOH}$ .

the neutral porphyrin core. The key similarity with the cationic hyperporphyrins described above appears to be that in both the cationic and anionic cases, the porphyrin is at a higher potential (i.e., more positively charged) than the phenyl substituents.

#### (b) Resonance Raman Spectroscopy of Hyperporphyrins.

Given that the special features of the hyperporphyrin spectra described above reflect phenyl-to-porphyrin CT transitions,<sup>10</sup> we wondered whether hyperporphyrins might also exhibit distinctive features in their RR spectra, especially in relation to vibrations involving the  $\text{C}_{\text{meso}}-\text{C}_{\text{phenyl}}$  coordinate. We find that this is indeed so. As for many free-base tetraarylporphyrins (e.g.,  $\text{TPPH}_2$ ), the  $\nu_1$  band, which is the fully symmetric  $\text{C}_{\text{meso}}-\text{C}_{\text{phenyl}}$  stretching vibration, is typically very strong in the Soret-resonant Raman spectra of tetraphenylporphyrin derivatives exhibiting hyper electronic spectra (Table 2 and Figure 9). Thus, TFA solutions of the majority of free-base tetraphenylporphyrins studied ( $\text{TArPH}_2$ ;  $\text{Ar} = p\text{-X}-\text{C}_6\text{H}_4$ , where  $\text{X} = \text{F}, \text{H}, \text{CF}_3$ , and  $\text{NO}_2$ ) and MeOH/ $\text{Bu}_4\text{NOH}$  solutions of  $T(p\text{-OH-P})\text{PH}_2$  and  $\text{Ni}[T(p\text{-OH-P})\text{P}]$  all exhibit a very intense  $\nu_1$  band at approximately  $1240\text{ cm}^{-1}$ .

Against this context, consistent with the nonhyper character of the electronic spectra of  $T(p\text{-NH}_2\text{-P})\text{PH}_2$  and  $\text{TPFPPH}_2$  in TFA, the  $\nu_1$  RR peak of these TFA solutions is very weak (Figure 9b).

**TABLE 2: Qualitative Intensity of the  $\nu_1$  RR Band for Tetraphenylporphyrins in Neutral (Usually Dichloromethane; Methanol for  $\text{Ni}[T(p\text{-OH-P})\text{P}]$ ), Acidic (TFA), or Basic (12.5%  $\text{Bu}_4\text{NOH}$  in Methanol) Solutions<sup>a</sup>**

porphyrin	neutral	acidic	basic
$\text{TPPH}_2^b$	++	++	N/A
$T(p\text{-F-P})\text{PH}_2$	N/M	+	N/A
$T(p\text{-CF}_3\text{-P})\text{PH}_2$	N/M	++	N/A
$T(p\text{-NO}_2\text{-P})\text{PH}_2$	N/M	++	N/A
$\text{TPFPPH}_2$	N/M	—	N/A
$T(p\text{-NH}_2\text{-P})\text{PH}_2$	N/M	—	N/A
$\text{OETPPH}_2$	++	++	N/A
$\text{Ni}[\text{OETPP}]$	—	N/A	N/A
$\text{Br}_8\text{TPPH}_2$	++	++	N/A
$\text{Cl}_8\text{TPPH}_2$	++	++	N/A
$T(p\text{-OH-P})\text{PH}_2$	N/M	N/M	++
$\text{Ni}[T(p\text{-OH-P})\text{P}]$	+	N/A	++
$\text{Ni}[T(p\text{-CF}_3\text{-P})\text{P}]$	—	N/A	N/A
$\text{Ni}[\text{TPP}]^{23}$	—	N/A	N/A
$\text{Ni}[\text{Br}_8\text{TPP}]$	—	N/A	N/A
$\text{Ni}[\text{Br}_8\text{TPP}(\text{Py})_2]$	++	N/A	N/A

<sup>a</sup> Symbols: — = low intensity, + = medium intensity, and ++ = strong intensity; N/A = not applicable and N/M = not measured. <sup>b</sup> The measurement was done in benzene instead of in dichloromethane.<sup>25</sup>

It may be noted that the  $\nu_1$  RR peaks of Ni tetraarylporphyrins, which are considered as hypso-porphyrins<sup>10</sup> on account of their relatively blue-shifted electronic spectra compared with free-base porphyrins, are relatively weak. In particular, the  $\nu_1$  RR peaks of saddled Ni tetraarylporphyrins are almost completely suppressed (Figure 9g). The following are some specific observations on Ni tetraarylporphyrins.

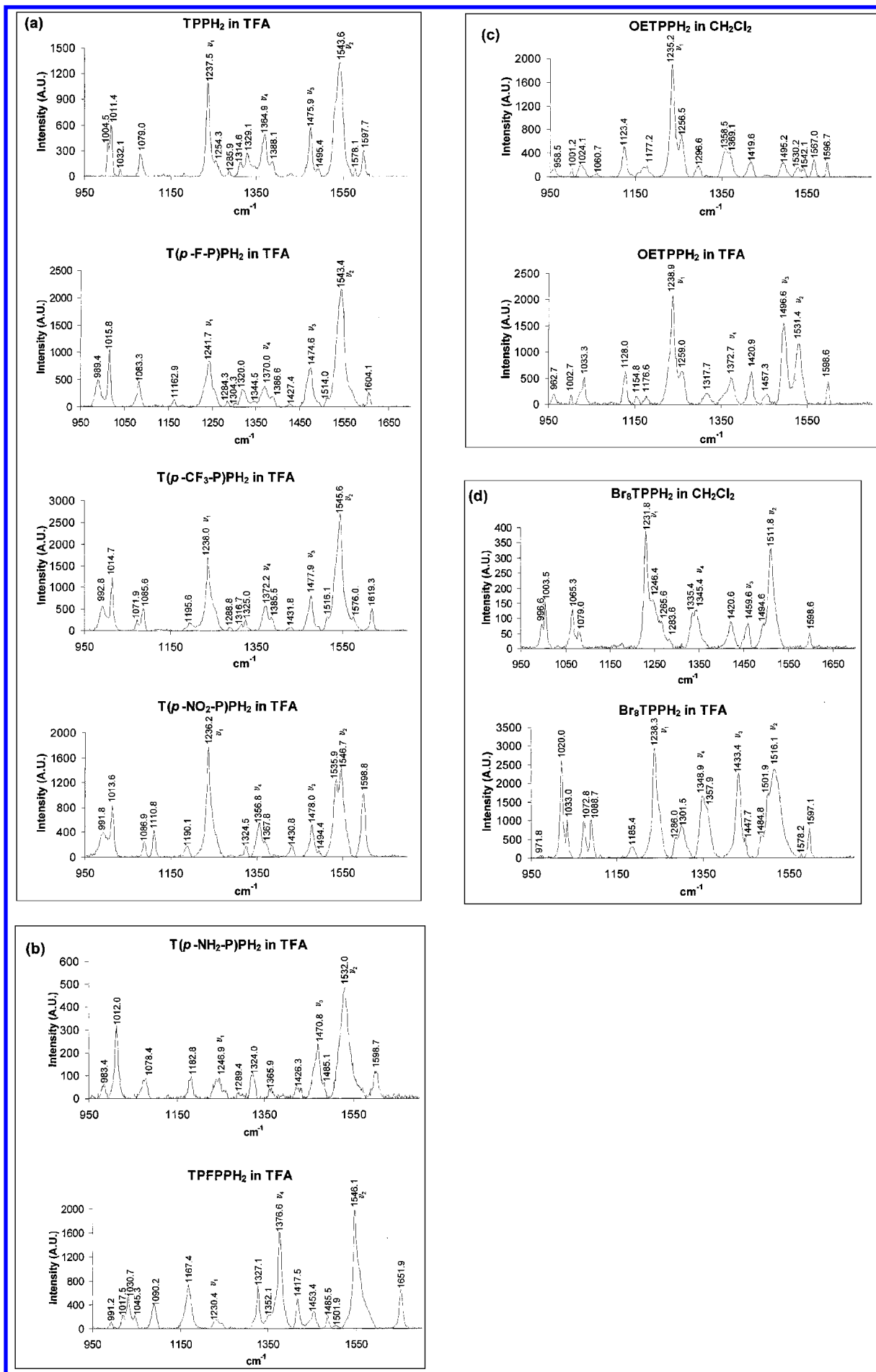
For  $T(p\text{-OH-P})\text{PH}_2$  and  $\text{Ni}[T(p\text{-OH-P})\text{P}]$ , the RR frequencies are nearly identical under neutral (methanol) versus basic (12.5% methanolic  $\text{Bu}_4\text{NOH}$ ) conditions (Figure 9f and g). The  $\nu_1$  peak of the electron-rich  $\text{Ni}[T(p\text{-OH-P})\text{P}]$  (Figure 9g) is reasonably strong under neutral conditions, compared with  $\text{Ni}[\text{TPP}]^{23}$  and  $\text{Ni}[T(p\text{-CF}_3\text{-P})\text{P}]$  (Figure 9g), but it does intensify significantly under basic conditions, consistent with the hyperporphyrin character of the basic solutions.

As we suggested elsewhere,<sup>24</sup> the intensity (but not the frequency) of the  $\nu_1$  feature appears to depend rather sensitively on the electronic character of the porphyrin macrocycle. For example, while the  $\nu_1$  feature is very weak for  $\text{Ni}[\text{Br}_8\text{TPP}]$ , it is intense for its  $S = 1$  bis(pyridine) adduct,  $\text{Ni}[\text{Br}_8\text{TPP}(\text{pyridine})_2]$  (Figure 9e), as well as for  $\text{Zn}[\text{Br}_8\text{TPP}]$  and  $\text{Cu}[\text{Br}_8\text{TPP}]$ .<sup>24</sup> The  $\nu_1$  feature of  $\text{Ni}[\text{OETPP}]$  is also moderately weak. It appears that occupancy of the metal  $d_{x^2-y^2}$  orbital as well as the electron-richness or otherwise of the saddled porphyrin ligand (e.g.,  $\text{Ni}[\text{Br}_8\text{TPP}]$  versus  $\text{Ni}[\text{OETPP}]$ ) plays a critical role in determining the intensity of the  $\nu_1$  feature.

**(c) A Note on the Electronic Absorption Spectra of Nonplanar Porphyrins.** Most nonplanar porphyrins, including the few studied in this work, exhibit significantly red-shifted spectra under ordinary, “nonhyper” conditions. In recent years, the origin of these red shifts has provoked considerable controversy, and therefore, we considered it worthwhile to provide a brief summary of the rather convoluted “story” vis-à-vis this issue.

Based on a large body of evidence, most porphyrin researchers believe that nonplanar distortions exert a significant effect on the redox and spectroscopic properties of porphyrins. However, in 1995, on the bases of electronic absorption spectroscopy and semiempirical AM1 calculations of *meso*-tetrakis(perfluoroalkyl)porphyrins, DiMaggio and co-workers challenged this prevailing view.<sup>11</sup> The Q and the B (Soret) bands of  $\beta$ -octahalogeno-*meso*-tetraarylporphyrins exhibit large red





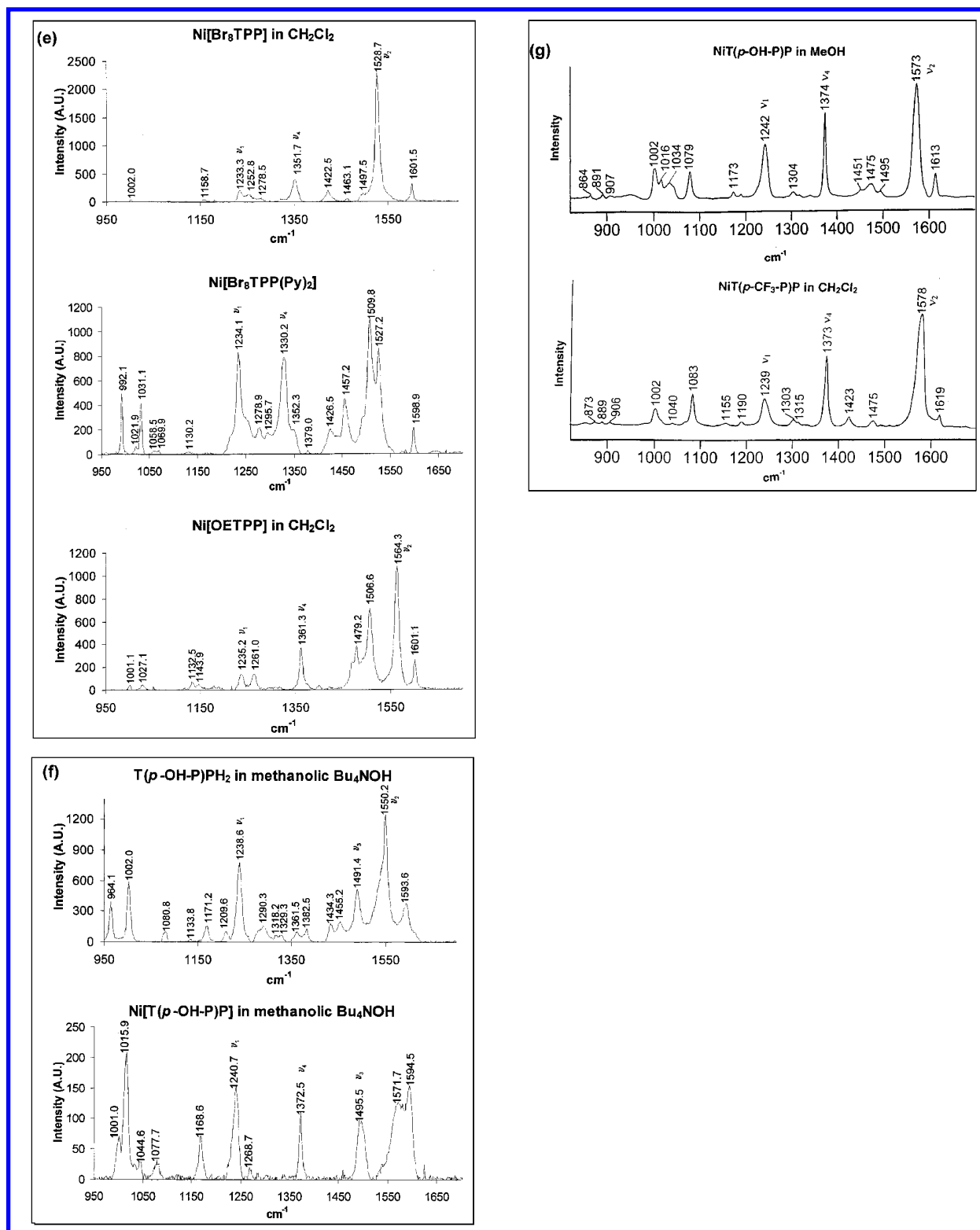


**Figure 9.** Soret-resonant Raman spectra of selected tetraarylporphyrins in different solutions ( $\lambda_{\text{ex}} = 457.9$  nm, 1 mV laser power unless specified otherwise). (a) TPPH<sub>2</sub>, T(*p*-F-P)PH<sub>2</sub>, T(*p*-CF<sub>3</sub>-P)PH<sub>2</sub>, and T(*p*-NO<sub>2</sub>-P)PH<sub>2</sub>; (b) T(*p*-NH<sub>2</sub>-P)PPH<sub>2</sub>, and TPFPPH<sub>2</sub>; (c) OETPPH<sub>2</sub>; (d) Br<sub>8</sub>TPPH<sub>2</sub> ( $\lambda_{\text{ex}} = 488.0$  nm, 1 mV laser power); (e) Ni[Br<sub>8</sub>TPP], Ni[Br<sub>8</sub>TPP(Py)<sub>2</sub>], and Ni[OETPP]; (f) T(*p*-OH-P)PH<sub>2</sub> and Ni[T(*p*-OH-P)P] ( $\lambda_{\text{ex}} = 406.0$  nm, 1 mV laser power) and Ni[T(*p*-CF<sub>3</sub>-P)P] ( $\lambda_{\text{ex}} = 406.0$  nm, 1 mV laser power).

shifts on the order of 30–52 nm, relative to the corresponding  $\beta$ -unsubstituted *meso*-tetraarylporphyrins. DiMaggio and co-workers argued that<sup>11</sup> “Saddle distortions allow (otherwise nearly orthogonal) aryl groups to rotate substantially into the plane of the [porphyrin] ring and interact more strongly with the  $\pi$ -system.” They posited “that the observed red shifts are not intrinsic to ring distortion, but result from different substituent

effects in planar and nonplanar conformations. This interpretation is bolstered by the observation that [*meso*-tetrakis(perfluoroalkyl)porphyrins and] dodecaalkylporphyrins, despite their large nonplanar distortions, show small shifts in their absorption spectra”.<sup>11</sup>

For a number of years, DiMaggio and co-workers’ proposal was neither confirmed nor challenged; on the basis of personal

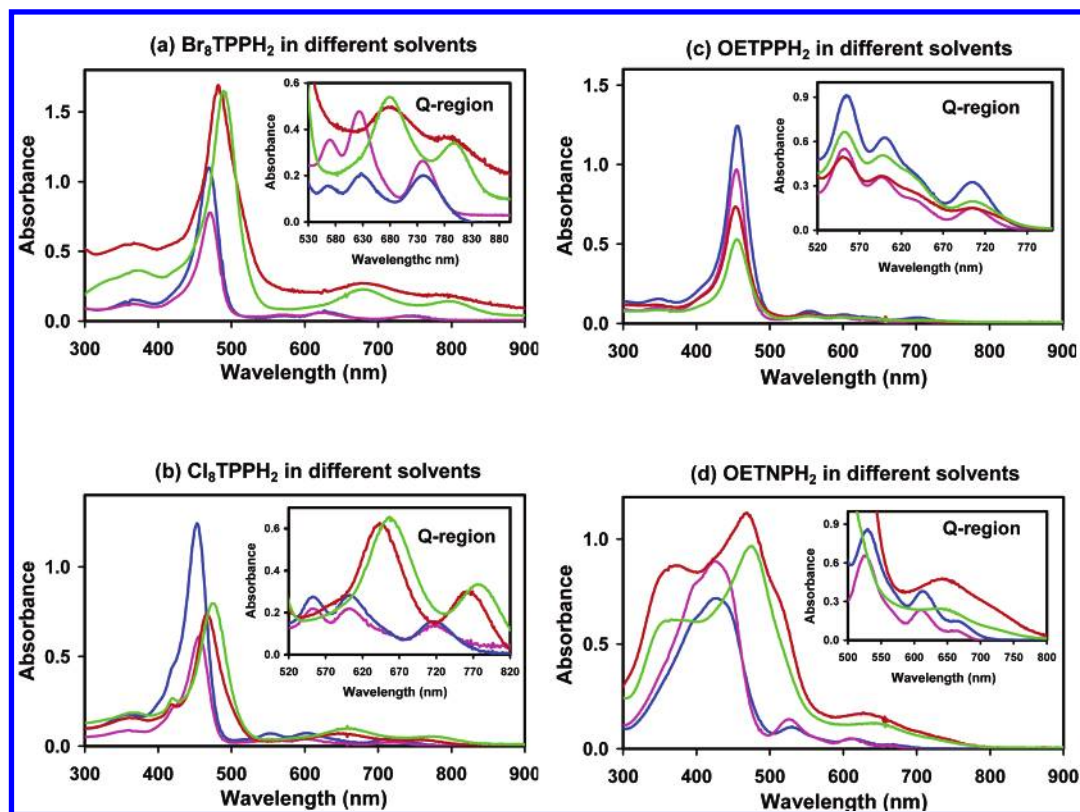


**Figure 10.** UV-vis spectra of selected saddled free-base porphyrins in dichloromethane (blue), toluene (magenta), dimethylformamide (red), and dimethylsulfoxide (green). (a) Br<sub>8</sub>TPPH<sub>2</sub>, (b) Cl<sub>8</sub>TPPH<sub>2</sub>, (c) OETPPH<sub>2</sub>, and (d) OETNPH<sub>2</sub>.

conversations with other researchers in the field, we understood that these findings were viewed with considerable skepticism and, therefore, were often ignored. In 2000, we<sup>12</sup> published a reinvestigation of this proposal using DFT/SCI calculations and reached conclusions opposite to that of DiMagno and co-workers, i.e., consistent with the traditional view that nonplanar distortions do bring about sizable red shifts in porphyrin electronic spectra. In a typical calculation,<sup>12</sup> we took the highly saddled optimized geometry of zinc  $\beta$ -octamethyl-*meso*-tetraphenylporphyrin and replaced the peripheral substituents with hydrogens lying exactly along the original C(porphyrin)-substituent vectors, setting the C(porphyrin)-H bonds to 1.08 Å. DFT/SCI calculations<sup>12</sup> on the artificially saddled ( $D_{2d}$ ) conformation of Zn porphine, thus obtained, yielded significantly red-shifted B and Q-bands, relative to those of the optimized planar ( $D_{4h}$ ) geometry of zinc porphine. Calculations such as these led us<sup>12</sup> to conclude that DiMagno and co-workers had reached an erroneous conclusion in their 1995 paper.<sup>12</sup> We wrote: "Presumably, the conclusions reached by DiMagno and co-workers reflect shortcomings of the semiempirical methods they used".<sup>12</sup>

In 2001, DiMagno and co-workers published a rebuttal to our 2000 paper.<sup>13</sup> Using constrained optimizations of simple free-base porphyrins where the degree of ruffling was the only constraint—an approach different from ours<sup>12</sup>—DiMagno and co-workers found little or no red shifts in the Q and B band energies calculated with time-dependent DFT(B3LYP)/6-311G\* (TDDFT) calculations.<sup>13</sup> This provokes two questions. How can we reconcile this finding with the incontrovertible fact that most nonplanar porphyrins do exhibit strongly red-shifted optical spectra? Second, given that both our<sup>12</sup> calculations and those of DiMagno<sup>13</sup> and co-workers are technically of high quality, what accounts for the dramatic difference in the results? DiMagno<sup>13</sup> and co-workers provided apparently satisfactory

**TABLE 3: UV-vis  $\lambda_{\text{Max}}$  in Solvents of Different Polarity of Nonplanar (saddled)  $\beta$ -Octa-Substituted-Porphyrins**

porphyrin	solvent	Soret bands <sup>a</sup>		red shift <sup>b</sup>	Q-bands		
Br <sub>8</sub> TPPH <sub>2</sub>	dichloromethane	369	469		571	626	744
	toluene	370	471	2	571	623	740
	dimethylformamide	372	483	14	680	786	
	dimethylsulfoxide	374	489	20	678	789	
Cl <sub>8</sub> TPPH <sub>2</sub>	dichloromethane	358	453		552	602	719
	toluene	358	456	3	553	601	716
	dimethylformamide	336	472	19	647	765	
	dimethylsulfoxide	365	475	22	660	781	
OETPPH <sub>2</sub>	dichloromethane	351	457		555	600	701
	hexane	354	452	-7	553	597	704
	pyridine	343	458	1	557	607	725
	toluene	349	455	-2	554	599	707
	dimethylformamide	349	455	-2	553	599	706
OETNPH <sub>2</sub>	dimethylsulfoxide	351	453	-4	554	600	707
	dichloromethane	397	427		531	614	667
	toluene	401	429	2	528	613	666
	dimethylformamide	361	471	44	514	645	
	dimethylsulfoxide	364	479	52	640		

<sup>a</sup> The second Soret band is the one of highest absorbance. <sup>b</sup> Red-shift of B-band with highest absorbance relative to dichloromethane.

answers to these questions. The main difference between our calculations<sup>12</sup> and those of DiMagno<sup>13</sup> and co-workers was that while we computed the electronic spectra of nonplanar porphine skeletons taken directly from the optimized structures of real nonplanar porphyrins, they carried out TDDFT calculations on fully optimized porphyrin structures, subject only to the constraint of various degrees of ruffling. DiMagno and co-workers provided evidence that it is not ruffling per se but changes in bond lengths and angles induced by the same substituents that bring about ruffling—what these authors call the in-plane nuclear



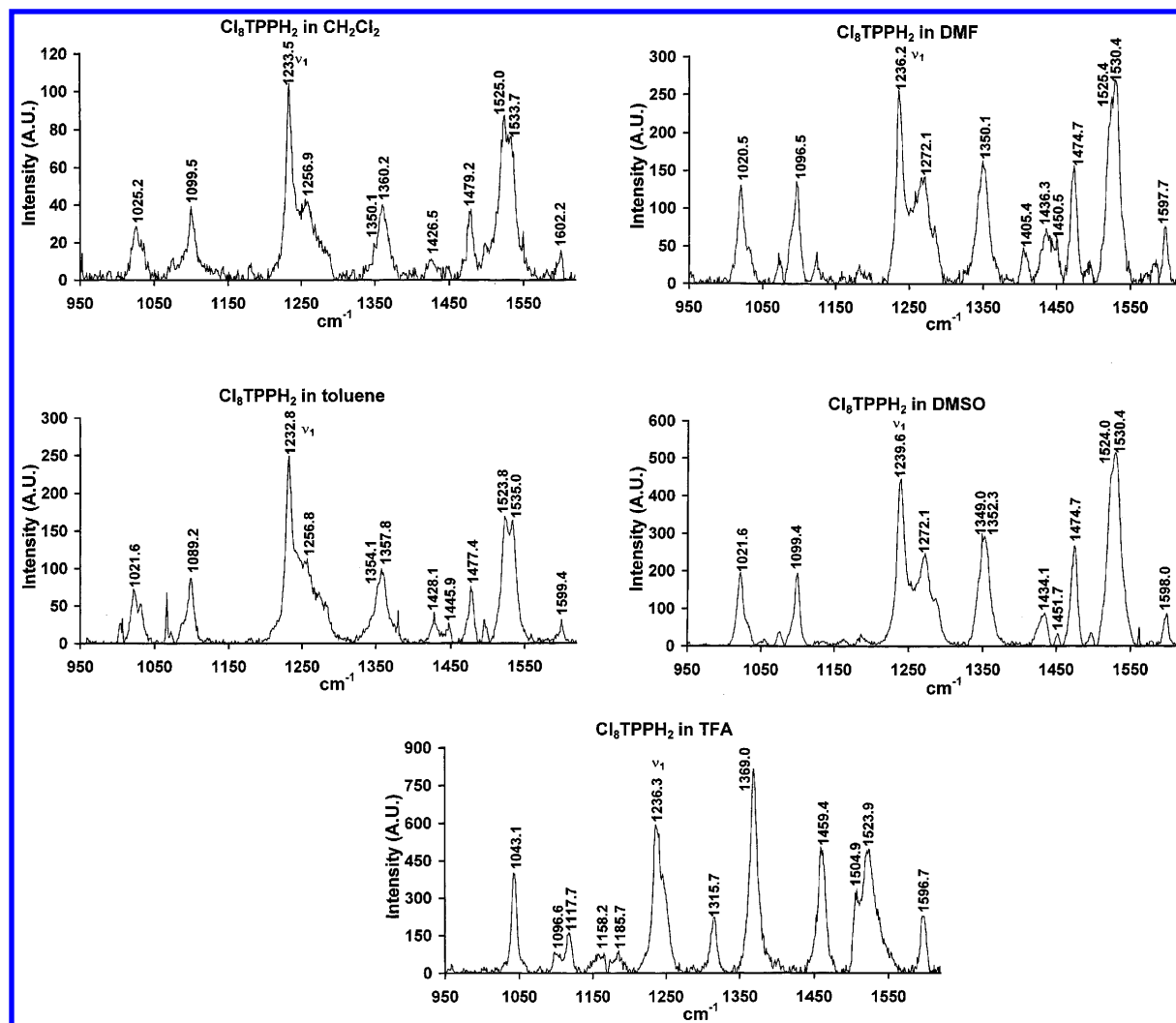


**Figure 11.** Resonance Raman spectra of the saddled free-base porphyrin  $\text{Cl}_8\text{TPPH}_2$  in different solvents: dichloromethane, toluene, dimethylformamide, dimethylsulfoxide, and trifluoroacetic acid ( $\lambda_{\text{ex}} = 457.9$  nm, 1 mV laser power).

reorganizations (IPNRs)—that play a key role in engendering the red shifts in the electronic spectra of nonplanar porphyrins.

In 2002, we again published a reexamination of DiMaggio and co-workers' work, this time acknowledging the correctness of these authors' findings. In our 2002 study, we carried out constrained geometry optimizations of a variety of free-base and metalloporphyrins, with the out-of-plane displacement of the *meso* (in the case of ruffled porphyrins) or  $\beta$  (in the case of saddled porphyrins) carbons as the only constraints and wrote: "We confirm DiMaggio and co-workers' finding that ruffling, *by itself*, does not engender significant red shifts in the Q and B band energies of simple porphyrins and metalloporphyrins, i.e., those that exhibit what Gouterman calls 'normal' optical spectra. We have now extended this finding to the saddling case, i.e., saddling too, *by itself*, does not bring about significantly red-shifted optical spectra. The phrase 'by itself' emphasizes that the red-shifted optical spectra exhibited by most nonplanar porphyrins do not actually result from nonplanarity, but from changes in bond distances and angles in the porphyrin skeleton—the IPNRs—brought about by substituents which also bring about the nonplanarity. Thus, it is possible to significantly ruffle and saddle a porphyrin without engendering sizable red shifts in its optical spectrum. As DiMaggio and co-workers have pointed out, this may be of relevance to relatively 'gentle' IPNR-free nonplanar distortion of a porphyrin cofactor within a protein matrix".<sup>14</sup>

However, very recently, Marchon, Medforth, Shelnutt and co-workers have implied<sup>15</sup> that we had in fact *not* erred in our conclusions in our 2000 paper. Indeed, our error appears to have been that, on the basis of the lack of red shifts for our artificial constrained-optimized nonplanar structures, we "jumped to the conclusion" in our 2002 paper<sup>14</sup> that the observed red-shifted optical spectra of real, substituted nonplanar porphyrins must result from the IPNRs proposed by DiMaggio and co-workers. What then accounts for the observed red shifts in the electronic spectra of nonplanar porphyrins? Marchon, Medforth, Shelnutt and co-workers provide computational evidence that the red shifts result not from structural displacements along the ruffling mode, but from displacements along *higher-frequency out-of-plane modes* that have the same symmetry as the ruffling mode. Presumably, the same scenario holds for saddled porphyrins. According to Shelnutt and co-workers, the specific geometrical factors responsible for the red shifts are changes in certain dihedral angles (e.g., the  $\text{N}-\text{C}_\alpha-\text{C}_{\text{meso}}-\text{C}_\alpha$  dihedral angle) involving the atoms in the porphyrin skeleton, but once again, for the sake of clarity, these do not correspond to either ruffling (and presumably also saddling) or IPNRs (i.e., significant changes in bond lengths and angles).

In summary, do nonplanar distortions account for a substantial part of the observed red shifts in the electronic spectra of various nonplanar porphyrins? The answer seems to be "yes," assuming the latest conclusions of Shelnutt and co-workers are correct.

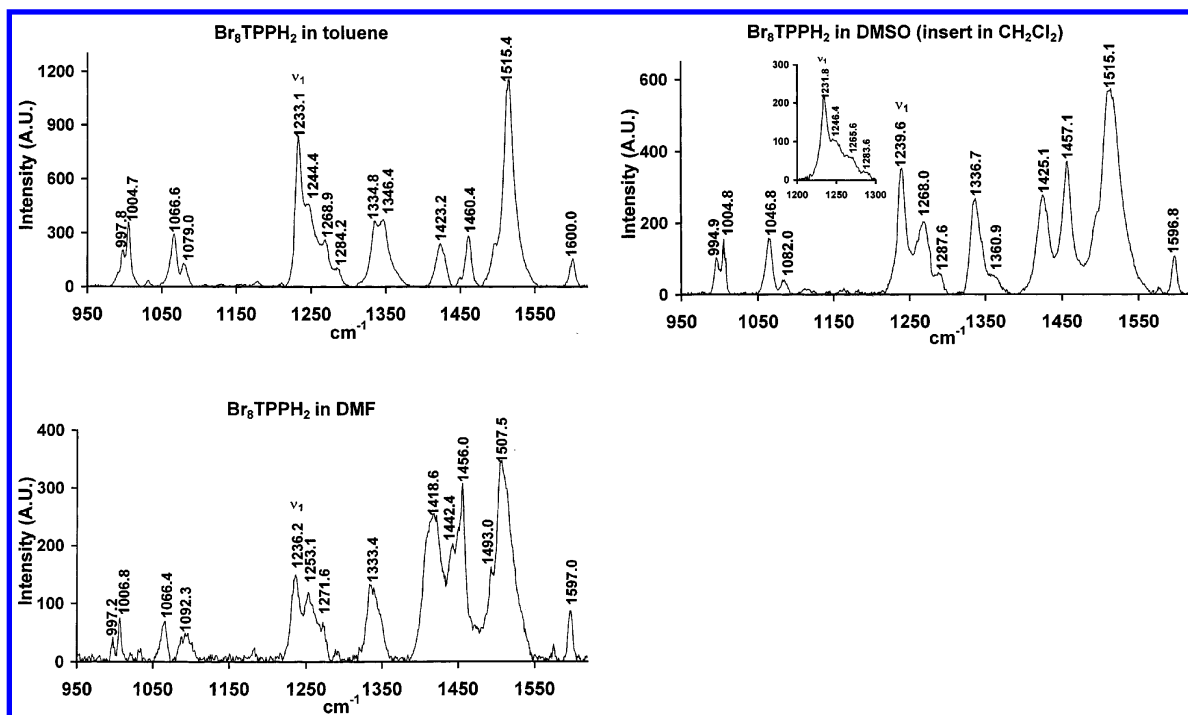


**Figure 12.** Resonance Raman spectra of the saddled free-base porphyrin  $\text{Br}_8\text{TPPH}_2$  in different solvents: toluene, dimethylformamide, dimethylsulfoxide, and dichloromethane ( $\lambda_{\text{ex}} = 457.9$  nm, 1 mW laser power).

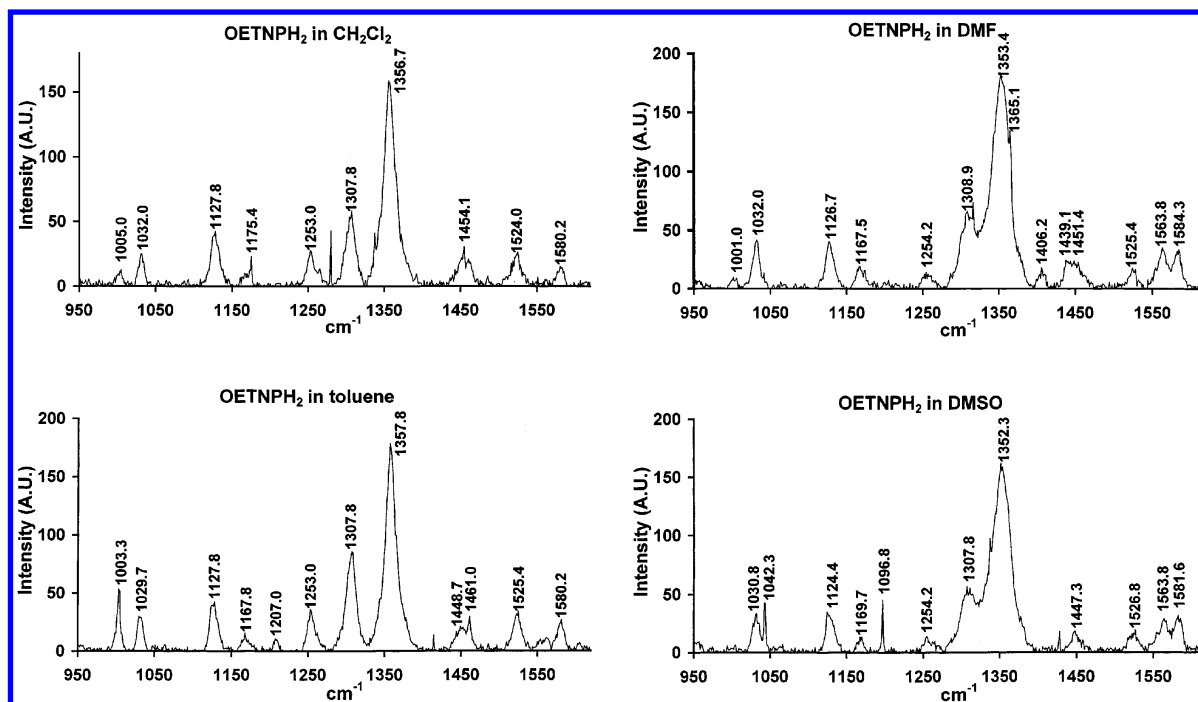


**Figure 13.** Resonance Raman spectra of the saddled free-base porphyrin  $\text{OETNPH}_2$  in different solvents: dichloromethane, toluene, dimethylformamide, and dimethylsulfoxide ( $\lambda_{\text{ex}} = 457.9$  nm, 1 mW laser power).

Does ruffling or saddling (interpreted narrowly as displacements along the ruffling and saddling modes) bring about significant red shifts? No. The solution to this paradox appears to be that the observed red shifts do not result from distortions along the so-called ruffling and saddling normal modes but from distortions along higher frequency modes that have the same symmetry as ruffling and presumably also saddling.

**(d) A Note on Solvent Effects on the Electronic Absorption Spectra of Nonplanar Porphyrins.** In general, the electronic absorption maxima of planar free-base porphyrins are relatively independent of the nature of the solvent<sup>16</sup> (barring strong acids

such as TFA). In contrast, the electronic absorption maxima of the saddled porphyrins  $\text{Br}_8\text{TPPH}_2$  and  $\text{Cl}_8\text{TPPH}_2$ <sup>17</sup> are strongly solvent-dependent, red-shifting with increasing solvent polarity. NMR studies suggest that these red shifts are due to hydrogen-bonding interactions involving the central NH groups of the saddled porphyrins and polar solvents such as DMF and DMSO.<sup>17</sup> As shown in Figure 10d, similar large solvent effects are also observed for  $\text{OETNPH}_2$ . In contrast, the electronic absorption maxima of  $\text{OETPPH}_2$  are essentially identical in toluene, dichloromethane, DMF, and DMSO (Figure 10c). These results might suggest that the strong solvent effects on the

electronic spectra are peculiar to relatively electron-deficient saddled porphyrins and are not observed for electron-rich saddled porphyrins such as OETPPH<sub>2</sub>. However, Takeda and Sato have reported that the electronic absorption spectrum of free-base dodecaphenylporphyrin (DPPH<sub>2</sub>)<sup>16</sup> red-shifts strongly in pyridine relative to a hexane solution. We found that the electronic absorption maxima of OETPPH<sub>2</sub> do red-shift slightly, by a few nanometers, in purified pyridine versus nonpolar solvents (Table 3). However, the red shifts can be much higher if the pyridine has not been carefully purified.

Bhyrappa and Bhavana have suggested that "The strong solvent-dependent UV–Visible spectral shift of haloporphyrin in polar solvents is due to an enhanced nonplanar distortion of the ring through hydrogen-bonding interactions between the core and the solvent molecules".<sup>17</sup> We argued that significant solvent-induced enhancements of macrocycle saddling should also be reflected in significant solvent-induced shifts in the RR spectra of the saddled porphyrins in question. However, Soret-resonant Raman measurements on Br<sub>8</sub>TPPH<sub>2</sub>, Cl<sub>8</sub>TPPH<sub>2</sub>, OETPPH<sub>2</sub>, and OETNPH<sub>2</sub> (Figures 11–13) did not reveal any significant solvent-induced shifts in any of the high-frequency marker bands in the 1300–1650 cm<sup>-1</sup> region, suggesting that the molecular geometry, including the degree of saddling, of the porphyrins is not significantly affected by the different solvents. The solvent-induced red shifts in the electronic absorption spectra therefore appear to be a largely electronic (as opposed to structural) effect, related to changes in the electronic character of the porphyrin ring as a result of hydrogen-bonding interactions with the solvent. The only significantly solvent-dependent RR feature of Br<sub>8</sub>TPPH<sub>2</sub> and Cl<sub>8</sub>TPPH<sub>2</sub> seems to be the  $\nu_1$  band, which upshifts by about 6 cm<sup>-1</sup> going from toluene to DMSO (Figures 11 and 12). This is consistent with our previous observation that the  $\nu_1$  band of tetraphenylporphyrin derivatives sensitively reflects the electronic character of the porphyrin ring.

## Conclusions

We have carried out a broad survey of tetraphenylporphyrin derivatives in relation to their possible hyperporphyrin character. The main conclusions of this study are as follows.

1. Most of the free-base tetraphenylporphyrins studied, i.e., TArPH<sub>2</sub>; Ar = *p*-X-C<sub>6</sub>H<sub>4</sub>, where X = CH<sub>3</sub>, H, CF<sub>3</sub>, and NO<sub>2</sub>, exhibit hyperporphyrin spectra in TFA solution (i.e. when centrally diprotonated). The hyper features are attributable to phenyl-to-porphyrin CT transitions.

2. Certain free-base tetraphenylporphyrins with very electron-deficient phenyl groups such as TPFPPH<sub>2</sub> do not exhibit hyperporphyrin spectra in TFA solution because, presumably, phenyl-to-porphyrin CT transitions involving extremely electron-deficient phenyl groups are not expected as prominent features in the optical spectra.

3. Anionic hyperporphyrins exist, as exemplified by T(*p*-OH-P)PH<sub>2</sub> or Ni[T(*p*-OH-P)] dissolved in methanolic Bu<sub>4</sub>NOH. The hyper transitions in these cases presumably involve CT from anionic phenolate substituents to the neutral porphyrin core.

4. To our knowledge, this is the first RR exploration of hyperporphyrins. Soret-resonant Raman spectra of various normal, hyper, and hypso tetraphenylporphyrin derivatives indicates the former two categories generally exhibit a more intense  $\nu_1$  band, which is the fully symmetric C<sub>meso</sub>–C<sub>phenyl</sub> stretching vibration, relative to hypso porphyrins such as square-planar nickel tetraarylporphyrins.

5. We have reinvestigated recent reports of large red shifts observed for the electronic spectra of saddled porphyrins in polar

solvents, an effect attributed to increased N–H···solvent hydrogen bonding in polar solvents. We find that such solvent-induced red shifts are observed for the relatively electron-deficient porphyrins Br<sub>8</sub>TPPH<sub>2</sub>, Cl<sub>8</sub>TPPH<sub>2</sub> and OETNPH<sub>2</sub> but not for the relatively electron-rich OETPPH<sub>2</sub>.

6. Resonance Raman spectra of free-base saddled porphyrins in different solvents reveal little shift in the high-frequency marker bands, which is consistent with little change in macrocycle conformation with solvent polarity. The observed solvent-induced red shifts in the electronic spectra therefore appear to reflect a largely electronic (as opposed to conformational) effect of N–H···solvent hydrogen bonding in polar solvents.

7. Finally, we have also presented a chronological summary of the controversial question as to whether nonplanar deformations are actually responsible for the red-shifted electronic spectra of the majority of nonplanar porphyrins.

**Acknowledgment.** We acknowledge financial support from the Norwegian Research Council and the VISTA program of the Norwegian Academy of the Sciences and Letters and Statoil (Norway). We thank Professor David Bocian for providing access to a Kr laser for certain of the RR measurements and Dr. Anwar for assistance with these experiments.

## References and Notes

- (1) Scheer, H., Ed. *Chlorophylls*, CRC Press: Boca Raton, FL, 1991; pp 3–1257.
- (2) Allen, C. M.; Sharman, W. M.; Van Lier, J. E. *J. Porphyrins Phthalocyanines* **2001**, 5, 161–169.
- (3) Phillips, D. *Prog. Reaction Kinet.* **1997**, 22, 175–300.
- (4) Zhou, R.; Josse, F.; Gopel, W.; Ozturk, Z. Z.; Bekaroglu, O. *Appl. Organomet. Chem.* **1996**, 10, 557–577.
- (5) Araki, K.; Angnes L.; Toma H. E. *Adv. Mater.* **1995**, 7, 554–559.
- (6) Mingotaud, A. F.; Mingotaud, C.; Patterson, L. K. *Thins Solid Films* **1992**, 210, 766–768.
- (7) Nakajima, R.; Yamazaki, I.; Griffith, B. W. *Biochem. Biophys. Res. Commun.* **1985**, 128, 1.
- (8) Dawson, J. H.; Sono, M.; Eble, K. S.; Hager, L. P. *Rev. Port. Quim.* **1985**, 27, 205.
- (9) Carbonmonoxycytochrome P<sub>450</sub> may be regarded as the classic bioinorganic hyperporphyrin, see: Hanson, L. K.; Eaton, W. A.; Sligar, S. G.; Gunsalus, I. C.; Gouterman, M.; Connell, C. R. *J. Am. Chem. Soc.* **1976**, 98, 2672–2674.
- (10) Gouterman, M. In *The Porphyrins*; Dolphin, D., Ed.; Academic: New York, 1978; Vol III, Chapter 1, pp 1–128.
- (11) DiMagno, S. G.; Wertsching, A. K.; Ross, C. R. *J. Am. Chem. Soc.* **1995**, 117, 8279.
- (12) Parusel, A. B. J.; Wondimagegn, T.; Ghosh, A. *J. Am. Chem. Soc.* **2000**, 122, 6371.
- (13) Wertsching, A. K.; Koch, A. S.; DiMagno, S. G. *J. Am. Chem. Soc.* **2001**, 123, 3932–3939.
- (14) Ryeng, H.; Ghosh, A. *J. Am. Chem. Soc.* **2002**, 124, 8099–8103.
- (15) Haddad, R. E.; Gazeau, S.; Pecaut, J.; Marchon, J.-C.; Medforth, C. J.; Shelnutt, J. A. *J. Am. Chem. Soc.* **2003**, 125, 1253–1268.
- (16) Takeda, J.; Sato, M. *Chem. Lett.* **1995**, 971.
- (17) Bhyrappa, P.; Bhavana, P. *Chem. Phys. Lett.* **2001**, 342, 39–44.
- (18) Ghosh, A.; Halvorsen, I.; Nilsen, J. H.; Steene, E.; Wondimagegn, T.; Lie, R.; van Caemelbecke, E.; Guo, N.; Ou, Z.; Kadish, K. M. *J. Phys. Chem.* **2001**, B105, 8120–8124.
- (19) Watanabe, E.; Nishimura, H.; Ogoshi, H.; Yoshida, Z. *Tetrahedron*, **1975**, 31, 1385–1390.
- (20) Vitasovic, M.; Gouterman, M.; Linschitz, H. *J. Porphyrins Phthalocyanines* **2001**, 5, 191–197.
- (21) Ojadi, E. C. A.; Linschitz, H.; Gouterman, M.; Walter, R. I.; Lindsey, J. S.; Wagner, R. W.; Droupadi, P. R.; Wang, W. *J. Phys. Chem.* **1993**, 97, 13192–13197.
- (22) Manna, B. K.; Bera, S. C.; Rohatgi-Mukherjee, K. K. *Spectrochim. Acta A* **1995**, 51, 1051–1060.
- (23) Jentzen, W.; Unger, E.; Song, X.; Jia, S.; Turowska-Tyrk, I.; Schweitzer-Stenner, R.; Dreybrodt, W.; Scheidt, W. R.; Shelnutt, J. A. *J. Phys. Chem. A* **1997**, 101, 5789–5798.
- (24) Halvorsen, I.; Steene, E.; Ghosh, A. *J. Porphyrins Phthalocyanines* **2001**, 5, 721–730.
- (25) Stein, P.; Ulman, A.; Spiro, T. G. *J. Phys. Chem.* **1984**, 88, 369–374.